Journal of Nuclear Materials 131 (1985) 99–104
North-Holland, Amsterdam

IMPROVEMENTS IN THE DESIGN AND ANALYSIS OF THE SEGMENTED EXPANDING MANDREL TEST

B.N. NOBREGA, J.S. KING and G.S. WAS

Department of Nuclear Engineering, The University of Michigan, Ann Arbor, MI 48109, USA

S.B. WISNER

General Electric Company, Vallecitos Nuclear Center, Pleasanton, CA 94566, USA

Received 6 August 1984; accepted 11 December 1984

The segmented expanding mandrel test is modified and improved to yield more quantitative information on the local stress and strain concentrations in Zircaloy tubing samples. The experimental apparatus has undergone changes in segment design, end restraint fixture design and the method of sample heating. These changes result in localization of stress and strain concentrations to known locations in the tubing, the introduction of a small degree of biaxiality and a more uniform sample temperature, respectively. A chamfered specimen design has been introduced for the purpose of producing a near plane-strain condition. Finite-element analysis has been added to provide information on the magnitude of localized stresses and strains given the sample geometry, test procedure and measured diametral strains. The resulting test represents a significant increase in the quantitative information produced in the segmented expanding mandrel technique.

1. Introduction

The segmented expanding mandrel test (SEMT) is a widely used laboratory technique for studying the pellet–clad interaction (PCI) phenomenon in Zircaloy tubing [1–3]. In one version of this test [1], a reactor-grade zirconium slug is compressed between metallic plungers at a constant rate in a mechanical testing machine. Four surrounding tungsten carbide (WC) segments are radially displaced against a continuous Al_2O_3 sleeve that simulates the UO_2 pellets. The sleeve breaks preferentially over the interface of the WC segments and the fragments load the tubing specimen in a way similar to the real situation. Thus, high local stresses and strains are imposed on four cladding regions by the radial displacement of the SEMT internal components.

The specimen diametral deformation over the midpoints of opposing segments is continuously measured, providing a signal for stopping the testing machine loading member when a desired strain is reached. The so-called "ramp and hold" (RH) testing mode, in which the strain is increased rapidly to a predetermined value and then held constant, provides a close simulation of power ramp effects in fuel cladding. The SEMT is also readily adaptable to test irradiated Zircaloy and can be performed in different chemical environments, namely flowing argon/iodine gaseous mixtures, solid and liquid cadmium, and saturated solutions of Cd in liquid Cs [4–6].

Thus, it would appear that the segmented expanding mandrel method is a qualitative simulation of the in-reactor case. However, conventional mandrel experiments have some limitations to their application as reliable sources of quantitative data. The most apparent limitation is that the all-important local mechanical specimen conditions are not easily determined with precision either experimentally or analytically. Moreover, the axiality of the local stresses is not well established. The low plastic failure strains typical of PCI-defected rods are not generally reproduced by SEMT simulations in either irradiated or unirradiated Zircaloy. Typical total diametral failure strains in SEMT specimens are greater than 2% [1,3,5]. Hence, the SEMT has traditionally been used as a screening test for Zircaloy cladding of different designs and conditions.

In this paper, we present modifications to the SEMT design and analysis methods that result in a test that has a biaxial stress state, better localization of stresses and strains, greater reproducibility and a more thorough knowledge of the stress and strain concentrations in the

0022-3115/85/$03.30 © Elsevier Science Publishers B.V.
(North-Holland Physics Publishing Division)

cladding during a ramp-hold test. This is achieved through the modification of test components, sample tubing design and analysis techniques.

2. Component modification

2.1. Segment design

Upon compression of the zirconium slug, the conventional segment design, shown in fig. 1, results in radial cracking of the Al_2O_3 sleeve around the entire circumference with preferential cracking occurring over the segment interfaces, fig. 2. Although the majority of the cracking occurs early in the loading sequence, some cracking may occur throughout the test. Therefore, the sites of the local stress and strain concentrations are constantly changing. The ramp test is thus actually a simulation of crack opening as well as crack formation which is not typical of the great majority of in-service ramps. Furthermore, the exact locations of segment fracture sites are ill-defined, thus preventing accurate modeling of the test.

An alternative design uses Al_2O_3 segments that retain a 445 μm gap between them when assembled around the zirconium slug, fig. 3. A similar design was used by Wood [7] in conjunction with a welded end-restraint fixture. The use of Al_2O_3 segments precludes the need for a sleeve. The change in internal components is advantageous for three reasons: (1) it allows the simulation of fuel crack opening (not formation) during power ramps; (2) it defines the exact geometry of the ceramic fragments that interact with the specimens which allows a more accurate finite-element representation of the test; and (3) it eliminates the WC segments and their potential for contaminating the test environment with extraneous iodides.

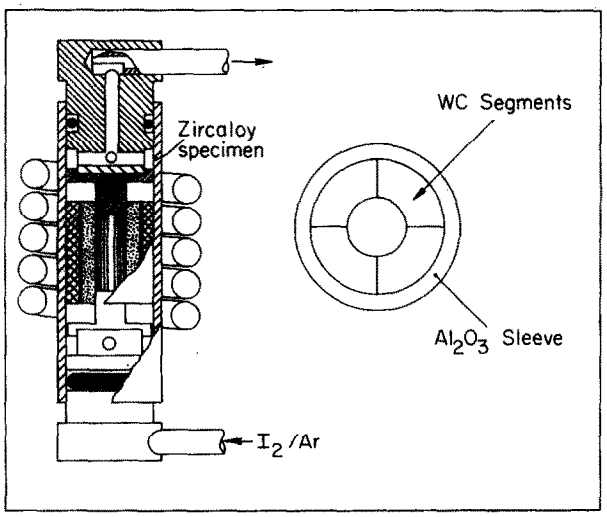

Fig. 1. Schematic of the segmented expanding mandrel test.

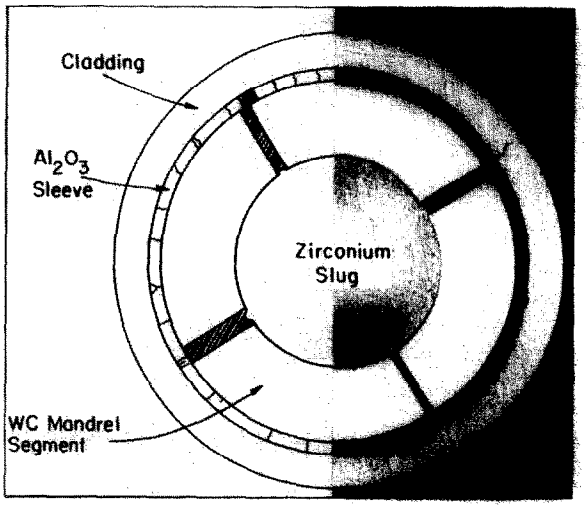

Fig. 2. Typical cracking pattern in the Al_2O_3 sleeve used in the conventional SEMT.

Although superior in terms of stress and strain localization, this design has a problem at large ramp strains. Large drops in axial strain are noted in samples instrumented with strain guages. These large strain releases are caused by the cracking of the ceramic segments as the specimens are ramped beyond a certain diametral strain; see fig. 4.

However, this design does result in a reduction in failure time which is caused by more severe loading conditions imposed by the thick segments. The number of Al_2O_3 segments is variable and an accurate simulation of in-reactor PCI would require some 16 segments [8,9]. Although some cracking does occur in the Al_2O_3 segments, this design is significantly more effective than the conventional design in localizing stresses and strains at known sites during ramp tests.

2.2. End-restraint fixture, ERF

In an effort to introduce a biaxial state of stress in the cladding, a fixture was designed to restrain the tube from axial shrinkage during the test. The fixture, shown in fig. 5, consists of two heavy stainless steel plates separated by four studs and clamped to the tubing

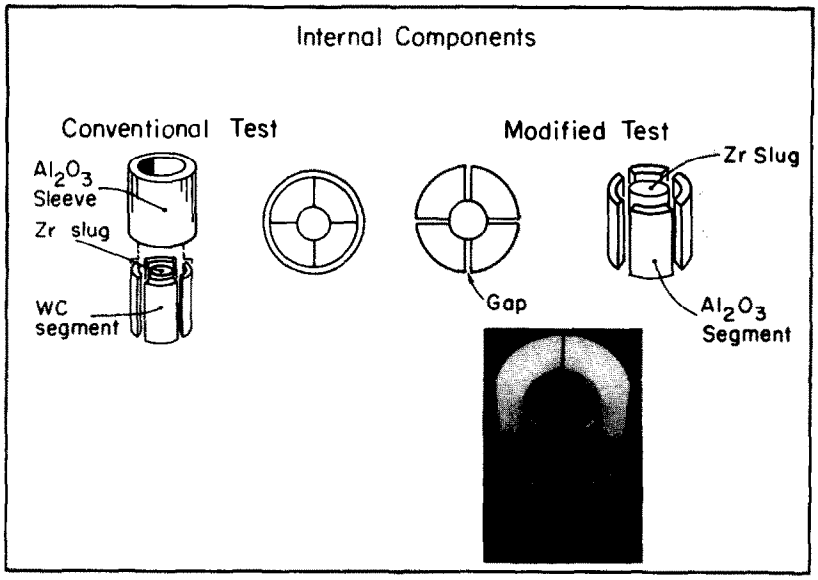

Fig. 3. Internal components in the conventional and modified SEMT.

sample by set screws. Tests made with samples instrumented with strain gauges and using the ERF indicate that a slight degree of biaxiality is introduced. This is determined by a decrease in axial strain in the restrained sample by about 10%. This is accompanied by a corresponding decrease in failure time but not in failure propensity.

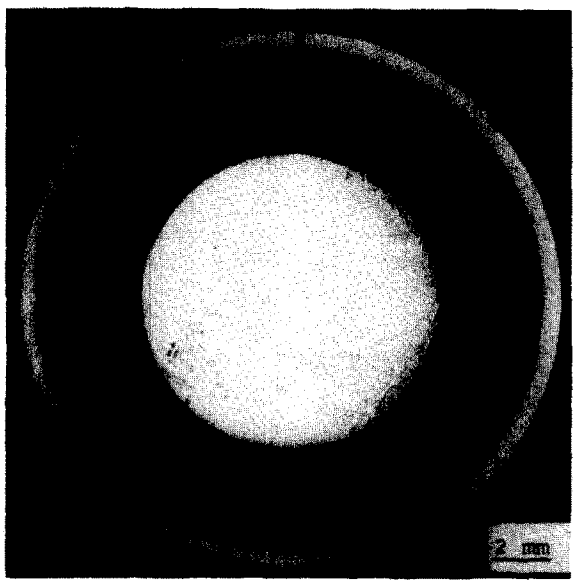

Fig. 4. Transverse cross-sections of a fractured, cold-worked, unirradiated specimen.

2.3. Resistance furnace

Conventional tests are conducted using a radio-frequency (RF) induction coil. This presents an inconvenient geometry when diametral strain measurements are desired. The perturbation of the RF heater coils that is necessary to accommodate a diametral extensometer results in an uneven temperature distribution in the sample. An alternative design uses a miniature resistance furnace, powered and monitored by a temperature controller. The set-up is shown in fig. 6 along with the ERF and diametral extensometer. Temperatures at the sample surface are considerably more uniform and are controlled to within $\pm 5°C$.

3. Sample design

A "chamfered" sample design is produced by milling four flats on the tubing outer diameter; see fig. 7. Milling was controlled so that the added cold work is limited to a depth of ~ 0.25 mm which will not affect SCC processes on the ID surface. The minimum thickness of the tube at the center of the flats is 445 μm, half the nominal tube thickness. The purpose of these flats is to establish a plane-strain state in the tube wall. The

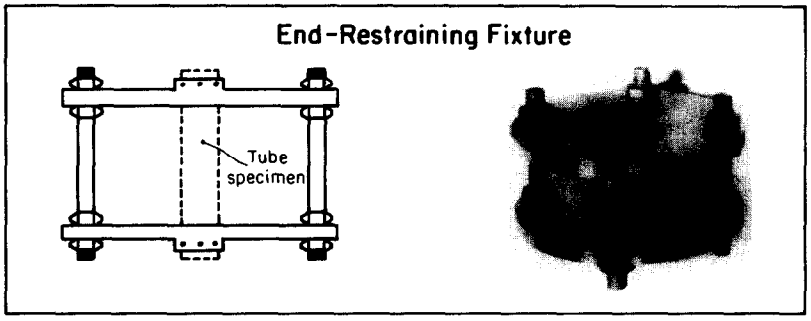

Fig. 5. Schematic of the end restraint fixture.

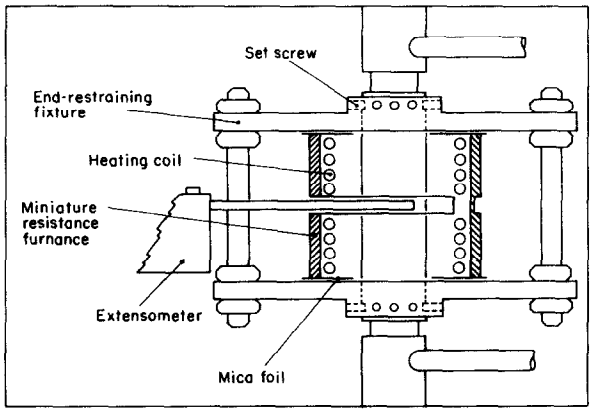

Fig. 6. Details of the complete, modified, segmented expanding mandrel test apparatus.

principle by which this occurs is analogous to the use of a reduced guage section in the plane-strain tensile test and results in a semi-plane-strain state in the clad. Samples instrumented with strain-guage rosettes and ramped to 0.8% diametral strain in room temperature air have an axial-to-hoop strain ratio of -0.21 compared with -0.46 for regular samples [10]. This is significantly closer to the plane-strain state ($\epsilon_z = 0$) than the true plane-stress state $\epsilon_z/\epsilon_\theta = -\nu = -0.43$. Diametral strain on both sample designs (regular and chamfered) is measured by fixing the extensometer contact points across the diameter connecting segment interfaces. Results of segmented expanding mandrel tests conducted on chamfered samples show that there is a significant drop in the measured diametral failure strain

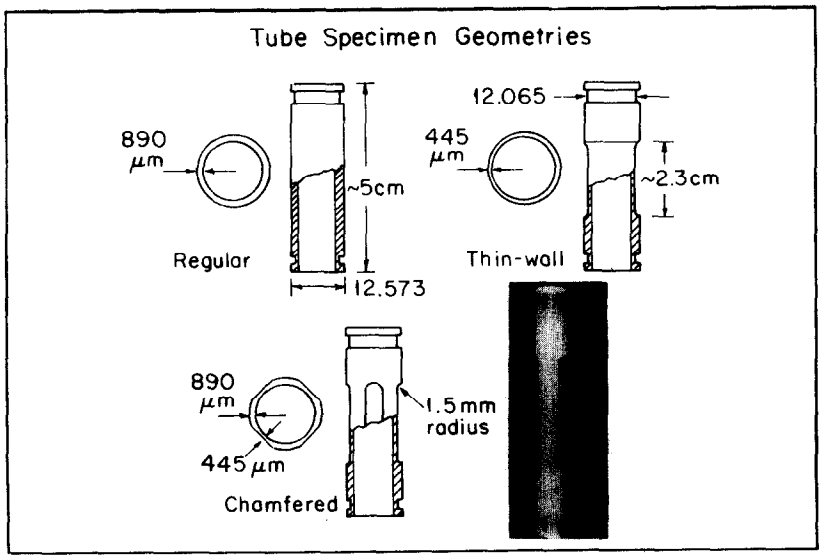

Fig. 7. Regular and chamfered tubing sample designs.

as compared with the regular tubing samples [10]. This is consistent with the effect of a plane-strain state.

4. Analysis

Of key importance in stress corrosion cracking tests is knowledge of the local stresses and strains at the crack site. The improvements discussed earlier provide for better identification of the location of these stress and strain concentrations, but direct measurements of these sites is nearly impossible. However, because the sites in the modified test are known beforehand, analytical modeling can be used to calculate the stress and strain concentrations given diametral strain measurements. Finite-element codes such as SAF2D [11,12] can be used to determine the stress–strain concentration during ramp-hold tests. SAF2D is a two dimensional finite-elements code, developed at General Electric, that is capable of modeling displacement-controlled loading, interfacial friction between the Al_2O_3 segments and the cladding, and cladding creep. The code accepts either axisymmetric (r–z) or transverse (r–θ) finite-element models. The latter requires either a plane stress ($\sigma_z = 0$), a plane strain ($\epsilon_z = 0$) or a generalized plane strain (ϵ_z = constant) condition. SAF2D models can comprise triangular, quadrilateral or special uniaxial elements. The latter can be used to simulate pellet–pellet and pellet–cladding contact including the effects of friction. Both the thermal and mechanical fuel and cladding responses are calculated.

Regular and chamfered tubing geometries are modeled as shown in fig. 8. Owing to the circumferential symmetry of the problem, only 45° sectors were modeled. The concentration of small (25 μm × 56 μm) quadrilateral elements in the cladding over the slit between adjacent Al_2O_3 segments minimizes numerical errors and improves the accuracy of the calculated local stresses and strains.

Ramp-hold SEMT tests were simulated by imposing 58 radial displacement increments (2 μm each) on node A, fig. 8, so that the displacement history of node B would match the measured laboratory test results. As described earlier, the extensometer measurements are made at node B.

Sliding boundary conditions were applied to the nodes on the AB symmetry line and to the cladding nodes on the 45° edge, that is these nodes were allowed to move radially only. The friction coefficient between the cladding and Al_2O_3 was assumed to be 0.55 as measured by Nakatsuka [13]. Both the plane-strain and plane-stress results were computed.

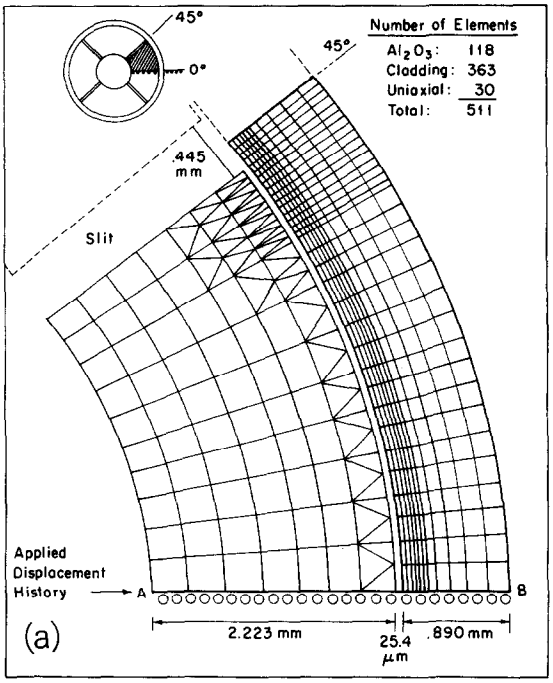

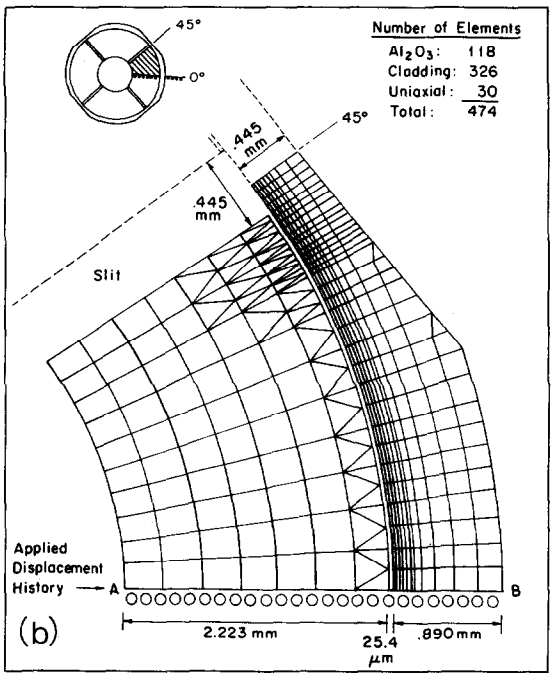

Fig. 8. The transverse finite element model of the (a) regular and (b) chamfered specimens.

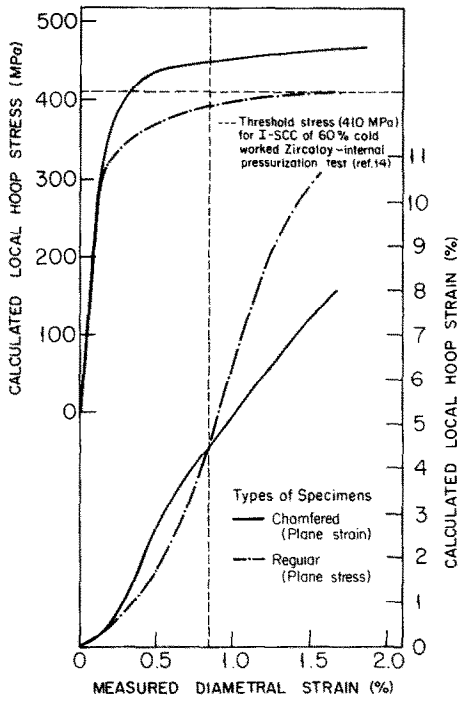

Fig. 9. Calculated local hoop stresses and strains on the inner surfaces of the two specimen designs at the segment interface corresponding to the measured diametral strain at the midpoint of the Al_2O_3 segment. Results shown assume a plane-stress state in the regular design and a plane-strain state in the chamfered design under isothermal conditions at 325°C.

The calculated local hoop stresses and strains on the inner surface of the cladding and over the Al_2O_3 interfaces are plotted in fig. 9 for regular samples modeled as plane-stress tests and chamfered samples modeled as plane-strain tests using the measured diametral strains as input to the calculations. The experimental RH tests are conducted at 325°C in 40 MPa iodine by moving the actuator (in compression) at 12.7 μm/min until a preset diametral strain is reached.

These results show an important aspect of the tests which would not be revealed without the modifications and finite-element analysis. The chamfered design results in a biaxial stress state which produces a larger local hoop stress for the same measured diametral hoop strain of 0.8% [10]. This results in the lower failure strains measured in tests on chamfered samples. Hence, by localizing the stress and strain concentration to specific, known sites and modeling the test with finite-element analysis methods, estimates of the magnitude of the local stress and strain concentrations can be made which can then be used to interpret test results.

5. Summary

The segmented expanding mandrel test has been modified to yield more accurate and detailed information on local stress and strain concentrations in tubing samples. Modifications were made to the experimental apparatus: improved segment design, implementation of an end restraint fixture and a new sample heating design; to the samples: development of a chamfered design to promote a plane strain state in the tubing; and analysis: use of finite-element analysis to yield information on the magnitude of local stress and strain concentrations.

Acknowledgements

The authors gratefully acknowledge R.P. Tucker, R.B. Adamson, G.H. Henderson, R.A. Rand and J.E. Lewis of the General Electric Company for their help in experiment design and data analysis.

References

[1] D.S. Tomalin, R.B. Adamson, and R.P. Gangloff, in: Zirconium in the Nuclear Industry, ASTM STP 681 (American Society for Testing and Materials, 1979) p. 122.
[2] A. Garlick, J. Nucl. Mater. 49 (1973/74), 209.
[3] R.P. Gangloff, GEAP-25093, General Electric Company, Schnectady, NY (Nov., 1979).
[4] F. Garzarolli, R. Manzel, M. Peeks and H. Stehle, Kerntechnik 20 (1978) p. 27.
[5] H.S. Rosenbaum, compiler, Demonstration of Fuel Resistant to Pellet-Cladding. Phase I. Final Report, GEAP-23773-2 (1979).
[6] S.B. Wisner and R.B. Adamson, presented at the Metallurgical Society of the AIME, St. Louis, Oct. 1982.
[7] J.C. Wood, J. Nucl. Mater. 57 (1975) 155.
[8] K. Videm and L. Lunde, Ann. Nucl. Energy 3 (1977) 305.
[9] Y.Y. Liu, Light-Water-Reactor Safety Research Program: Quarterly Progress Report, July–Sept. 1981, NUREG/CR-2437 Vol. III, ANL-81-77 Vol. III.
[10] B. Nobrega, R. Adamson, J. King and G. Was, J. Nucl. Mater. 131 (1985) 126, this issue.
[11] Y.R. Rashid, in: Proc. Conf. on Computational Methods in Nuclear Engineering (Charleston SC, 1975).
[12] Y.R. Rashid, Nucl. Engrg. Des. 29 (1974) 22.
[13] M. Nakatsuka, J. Nucl. Mater. 96 (1981) 205.
[14] K. Videm, L Lunde, T. Hollowell, K. Vilpponen and C. Vitanza, J. Nucl. Mater. 87 (1979) 259.